Histol Histopathol (2008) 23: 717-730

http://www.hh.um.es

Histology and Histopathology

Cellular and Molecular Biology

Cisplatin treatment of NIH/3T3 cultures induces a form of autophagic death in polyploid cells

Alessandra Spano[1], Gianni Monaco[1], Sergio Barni[2] and Luigi Sciola[1]

[1]Department of Physiological, Biochemical and Cellular Sciences, University of Sassari, Sassari, Italy and

[2]Department of Animal Biology and CNR Center for Histochemistry, Pavia, University of Pavia, Italy

Summary. The effects induced by different concentrations (50, 75, 100 μM) of the cytostatic drug cisplatin (cDDP) in NIH/3T3 cells were analyzed. Sub-confluent cultures of this mouse fibroblast line, obtained after serum deprivation, showed the presence of aneuploid/polyploid cells with ploidy values ranging from 4c to 24c. DNA content cytofluorometry demonstrated that 50 and 75 μM cDDP induced a cytostatic effect; 100 μM concentration showed lower antiproliferative action. All treatments caused a partial cell detachment and apoptosis, the incidence of which appeared to be cDDP concentration-dependent. Ultrastructural and fluorescence microscopy integrated analyses of the still adherent cells demonstrated the presence of alternative degeneration patterns, especially in polyploid cells, with extensive modifications at both nuclear and cytoplasmic levels. There were events of micronucleation and phenomena of multilobulation and furrows of the nucleus that preceded the formation of heterogeneous fragments. These events were correlated, at cytoplasmic level, with actin reorganization and the appearance of autophagocytotic processes. In our cell model, the same pharmacological treatment was able to induce different cell death phenomena relating to cell dimension and ploidy. More actively proliferating cells (2c–4c DNA content) die throughout canonical apoptosis, while polyploid cells prevailingly degenerate by mechanisms partly referable to autophagic cell death.

Key words: NIH/3T3 cells, Cisplatin, Cell kinetics, Polyploidy, Autophagic cell death

Offprint requests to: Luigi Sciola, Department of Physiological, Bichemical, Biological and Cellular Sciences, University of Sassari, Via Muroni, 25-I-07100 Sassari, Italy. e-mail: sciola@uniss.it

Introduction

In malignant tumors, and especially those that are well-differentiated, there is often a predominant cell population the DNA content of which is near the diploid value. This population constitutes the subfraction of more actively proliferating cells (Böhm and Sandritter 1975; Mora et al., 2007); in many cases, moreover, there are a number of cells whose ploidy is higher than that of the predominant or modal population. High-ploidy cells are present even in several immortalized cell cultures, tumor lines or incipient tumors and have long been singled out by pathologists, who regarded them as a clear sign of malignancy (Dejmek et al., 1992; Melchiorri et al., 1994). Although the biological significance of high-ploidy tumor cells has been already investigated in the past years (Liautaud-Roger et al., 1990; Baroja et al., 1996), to this day it is still not completely clear. Polyplodization is regarded as being a crucial step leading to aneuplody in tumor cells (Ciciarello et al., 2001; Nguen and Ravid, 2006; Yildirim-Assaf et al., 2007). In fact, tumors appear to arise as a consequence of proliferation/differentiation anomalies, genomic instability and karyological rearrangement (Klein and Klein 1985). Aneuplody is frequently subsequent to an intermediate tetraploid state and, in tumors, correlates with high malignancy, metastatic progression and poor prognosis (Andreassen et al., 2001). On the other hand, the heterogeneity of the tumor cell population can be partly responsible for the inefficacy of chemotherapic treatment and for the failure to eliminate some tumor cells. In fact, the different phenotypic features of the cells can play a crucial role in the sensitivity or in the different response to apoptosis-inducing pharmacological conditions (Sciola et al., 2003). From this perspective, it is important to gain further knowledge about the mechanisms of induction and dynamics of cell death in polyploid cells, in both experimental and pathological conditions.

In comparison to their diploid counterparts, in some cases, polyploid/aneuploid cancer cells can show a different reactivity to chemical agents dependent on differentiation (Spano et al., 2007) and exhibit an enhanced or decreased rate of death correlated with the existence of p53-dependent alterations in apoptosis regulation (Castedo et al., 2006).

Amongst DNA damaging drugs, cis-dichloro-diammineplatinum (cDDP) has been used effectively to treat various human cancer types; even though the precise mechanism underlying its cytotoxicity is not yet fully known, there is evidence that G1/S arrest induction is a critical step in cisplatin action (Un, 2007). Cell cycle arrest, in addition to DNA unrepair and inhibition of transcription, represents the main cytotoxic end point of the drug, leading to cell death (Siddik, 2003). Many reports have shown a link between mismatch repair deficiency and the loss of normal cell cycle control, and in particular the loss of G2 arrest (Strathdee et al., 2001). In response to DNA damage, the cellular decision between life and death involves an intricate network of factors that play critical roles in the regulation of DNA repair, cell cycle and cell death, and which can also be influenced by cell ploidy level (Zong et al., 1998). As is widely known, tumor cells display anomalies in their DNA content because of their cell cycle disarrangement and several pieces of evidence suggest that high-ploidy cells could be especially resistant to various aggressions; this late biological feature could be of great interest to cancer treatment (Baroja et al., 1998).

Starting from these considerations, in the present work, we have used a cell model constituted by a culture derived from NIH/3T3 mouse fibroblast line, obtained after prolonged serum deprivation; amongst these cells, re-fed with complete medium and in conditions of cell sub-confluence, polyploid cells with DNA content values ranging from 4c to 24c were seen to appear. The induction of polyploidy after serum withdrawal has been previously documented (Nishigaki et al., 2003). In our cell model, the appearance of polyploid cells can express genetic instability and sensitivity to cell transformation, which can be influenced by treatment with chemicals. To investigate these biological aspects and the relationship with cell death, we have incubated the cells for 24 h with increasing concentrations (50, 75 and 100 μM) of the chemotherapeutic agent cDDP, correlating the cytostatic and cell death effects with the different ploidy levels. The use of an experimental model, constituted by a heterogeneous cell population, could contribute to knowledge of the role of polyploid cells in the dynamics of neoplastic cell populations in tumors consisting of several polyploid cells.

Materials and methods

Cell cultures

The NIH/3T3 culture, used in this work, was obtained after prolonged (7-10 days) serum deprivation (culture medium containing 0.5% foetal calf serum) of this mouse embryo fibroblast line. The withdrawal of serum caused a massive cell detachment and death of almost all cells constituting the culture. A small fraction of surviving cells, when serum was restored, re-entered the cell cycle and, after recovery of the normal proliferative activity, showed a higher presence of polyploid cells than the original NIH/3T3 cultures.

In the experiments performed in this work, the cells were usually maintained in Dulbecco's modified Eagle's medium supplemented with 10% foetal calf serum, 2 mM L-glutamine, 100 units/ml penicillin, and 100 μg/ml streptomycin (Invitrogen Ltd., Paisley, UK). The cells were cultured at 37°C in a humidified chamber containing 5% CO_2, and analyzed, as sub-confluent monolayer, both in control and after treatment conditions.

Drug treatment

Cell cultures were treated (for 24 h) with a cytostatic agent, cis-dichlorodiammine-platinum (cDDP) (SIGMA, St. Louis, MO), at different concentrations (50, 75 and 100 μM) in complete medium.

Flow cytometry

Cell cycle and cell death incidence were analyzed by means of a PARTEC PAS II flow cytometer (PARTEC GmbH, Münster, DE).

Sub-confluent NIH/3T3 cells, before and after cDDP treatment, were collected, from T-25 cm^2 culture flasks, by trypsinization (trypsin 0.25% in PBS). After washing in PBS, the cells were fixed in 70% ethanol at 4°C for 30 minutes. The measurements of DNA/protein relative content were performed after fluorochromization (45 minutes at room temperature) with 8 μM DAPI (4',6-diamidino-2-phenylindole; SIGMA) and 50 μM SR 101 (Sulforhodamine 101; SIGMA) in 0.1 M Tris-HCl buffer pH 7.5, respectively, and at least 25000 cells were analyzed for each determination. The instrument equipped with an Hg lamp was used in the optic configuration for UV excitation (λ = 350 nm), for the simultaneous DAPI (λ = 435 nm) and SR 101 (λ = 630 nm) emission. The data were collected in frequency histograms of DNA content and DNA/protein cytograms.

The calculation of the percentage of the cells in the various cell cycle phases and in apoptosis was performed on frequency cumulative curves of DNA histograms. The estimation of conventional apoptotic cells was performed by considering the hypo-2c values. Comparison between the different experimental conditions was carried out using the Student's t-test and the differences were considered statistically significant with a $P < 0.05$.

Static cytometry

NIH/3T3 cells, grown on coverslips, were fixed with 70% ethanol for 30 min at 4°C. The amount of DNA per

cell was evaluated, after DAPI fluorochromization, by measuring the fluorescence emitted by each single nucleus. For this analysis, a cytoflurometer NIKON P II (NIKON, Kanagawa, JP) was used. In the cytometric apparatus, an appropriate system of diaphragms permitted the selection of single nuclei and the fluorescence was quantitatively analyzed after automatic subtraction of the background brightness.

For each experimental condition, three slides were examined and 300 cells per slide were measured. The results were represented as histograms of DNA content.

Fluorescence microscopy

Acridine Orange supravital staining

Vital NIH/3T3 cells, in control conditions and after cDDP treatment, were fluorochromized with Acridine Orange (SIGMA) (0.1% in complete medium) for 10 min at 37°C. Specimens were observed in epifluorescence with a NIKON Eclipse 600 microscope, by using blue light (488 nm) to excite simultaneously the nuclear green (λ_{em} = 520 nm), and the cytoplasmic red (λ_{em} = 590 nm) fluorescences.

Actin network labelling

After washing in PBS, cells, grown on glass coverslips, were fixed in 3% paraformaldheyde (PFA) in PBS containing 1 mM $CaCl_2$ and 1 mM $MgCl_2$ (Buffer A) for 30 min at room temperature. After fixation and washing in Buffer A, the cells were permeabilized with Triton X-100 (0.2% in Buffer A) for 15 min at room temperature.

Actin microfilament visualization was performed by incubating the cells in the presence of TRITC-conjugated phalloidin (SIGMA) (dilution 1:50) for 45 min in a humid chamber.

Nuclear counterstaining was obtained with Hoechst 33342 (2 µg/ml in PBS; SIGMA) for 10 minutes at room temperature. After washing in Buffer A, coverslips were mounted in 1:10 (v/v) mixture of PBS/glycerol containing p-phenylendiamine as antifading agent. Observation was performed by epifluorescence with a NIKON Eclipse 600 microscope equipped with a 100-W mercury lamp. The following conditions were used: 330-380 nm excitation filter (excf), 400 nm dichroic mirror (dm) and 420 nm barrier filter (bf) for Hoechst 33342; 540 nm excf, 580 nm dm and 590 nm bf for TRITC.

Transmission electron microscopy

NIH/3T3 cells, grown in 75 cm^2 culture flasks, in the various experimental conditions, were collected by centrifugation. Pellets were fixed with 2.5% glutaraldheyde in cacodylate buffer (0.1 M, pH 7.4) for 2 hours. After washing in cacodylate buffer containing 6% sucrose, the pellets were post-fixed in 1% OsO_4 in cacodylate buffer for 90 minutes at 4°C. The cells were then resuspended in 1 ml 2% agarose at 35°C and centrifuged at 300g for 10 minutes at 35°C. After 1 hour at 4°C, the samples were fragmented, dehydrated in an ethanol series and embedded in epoxy resin (Agar 100; Agar Scientific, Stansted Essex, UK) at 60°C for 48 hours. Ultrathin sections were double stained with uranyl acetate and lead citrate, examined and photographed using a Zeiss EM 900 transmission electron microscope (Carl Zeiss Jena GmbH, Jena, DE), operating at 80 kV.

Results

Effects on cell cycle and death induction

This study analysed the dynamics of cDDP-induced changes, relating to the whole population of NIH/3T3 cells, constituted by highly-proliferating (predominant cell component) and polyploid/aneuploid cells. Pharmacological effects on the cell cycle and death were correlated with cell ploidy levels, by an integrated analysis of DNA content, performed by flow (Fig. 1A,C,E,G) and static (Fig. 1B,D,F,H) cytometry. Cell protein content changes in different conditions of ploidy level were measured by biparametric flow cytometry (Fig. 2).

In control conditions, static cytometric measurements showed not only 2c (G1 phase in flow cytometry) and 4c (G2/M phase in flow cytometry) DNA content values, but also the presence of signals (ranging from 4c to 24c) relative to aneuploid/polyploid cells (Fig. 1B).

From a methodological point of view, flow cytometric measurements after cDDP treatment (Fig. 1C,E,G) refer to both floating cells, which were induced to detach by drug treatment, and the majority of adherent cells detached by trypsinization, while those performed by static cytometry (Fig. 1B,D,F,H) also included the residual adherent cells, constituted by highly-polyploid cells. The latter cells displayed strong adhesive capability and lower detachment by common methods used to obtain single cell suspension for flow cytometry. In this way, by combining the two cytometric approaches, the population of polyploid cells of our cell model is entirely represented.

In cDDP-treated cells, the analysis of the DNA content profiles obtained by flow cytometry indicated that the drug induced different dose-dependent cytokinetic changes, in the concentration range of 50-100 µM (Fig. 1). In particular, at concentrations of 50 and 75 µM, the cytostatic effect prevailed, while at 100 µM there was an increase in events of cell death. Furthermore, flow cytometry showed that all treatment conditions caused cell detachment with the appearance of the classical apoptotic profile represented by sub-G1 peak (Fig. 1C,E,G), the incidence of which appeared to be drug concentration-dependent. In all treatment conditions, the protein amount, in both diploid and polyploid/aneuploid cells, showed an evident decrease (Fig. 2). As far as the specific effects on the cell cycle phases of actively proliferating cell compartment were concerned, 50 µM cDDP induced a slowing down of the

cell progression toward the G2/M phase (4c cells), with a consequent accumulation of cells in the G1 phase (2c and 2-4c cells) and a decrease of G2/M cells (Fig. 1C). Treatment with 50 μM cDDP also caused a decrease of cells with ploidy values ranging from 6c to 14c, while those with higher ploidy (in proximity to 16c and to 22c) tended to increase (Fig. 1D). In particular, the evident decrease of 8c cells can be related not only to degenerative events, but also to a reduced number of tetraploid cells in the G2/M phase (Fig. 1C).

Treatment with 75 μM cDDP induced cytostatic/death effects, which can be due to the partial cell incapability to enter the S phase, and the increase of apoptosis in cells derived from those accumulated in the G1 phase of the cell cycle (sub-G1 peak in figure 1E).

Furthermore, at 75 μM dose, in comparison to 50 μM cDDP, an increase of 4c and 8c DNA values was also observed, as a probable consequence of the more intense effect of G1 block in tetraploid/octaploid cells (Fig. 1E). In addition to the loss of cells with ploidy

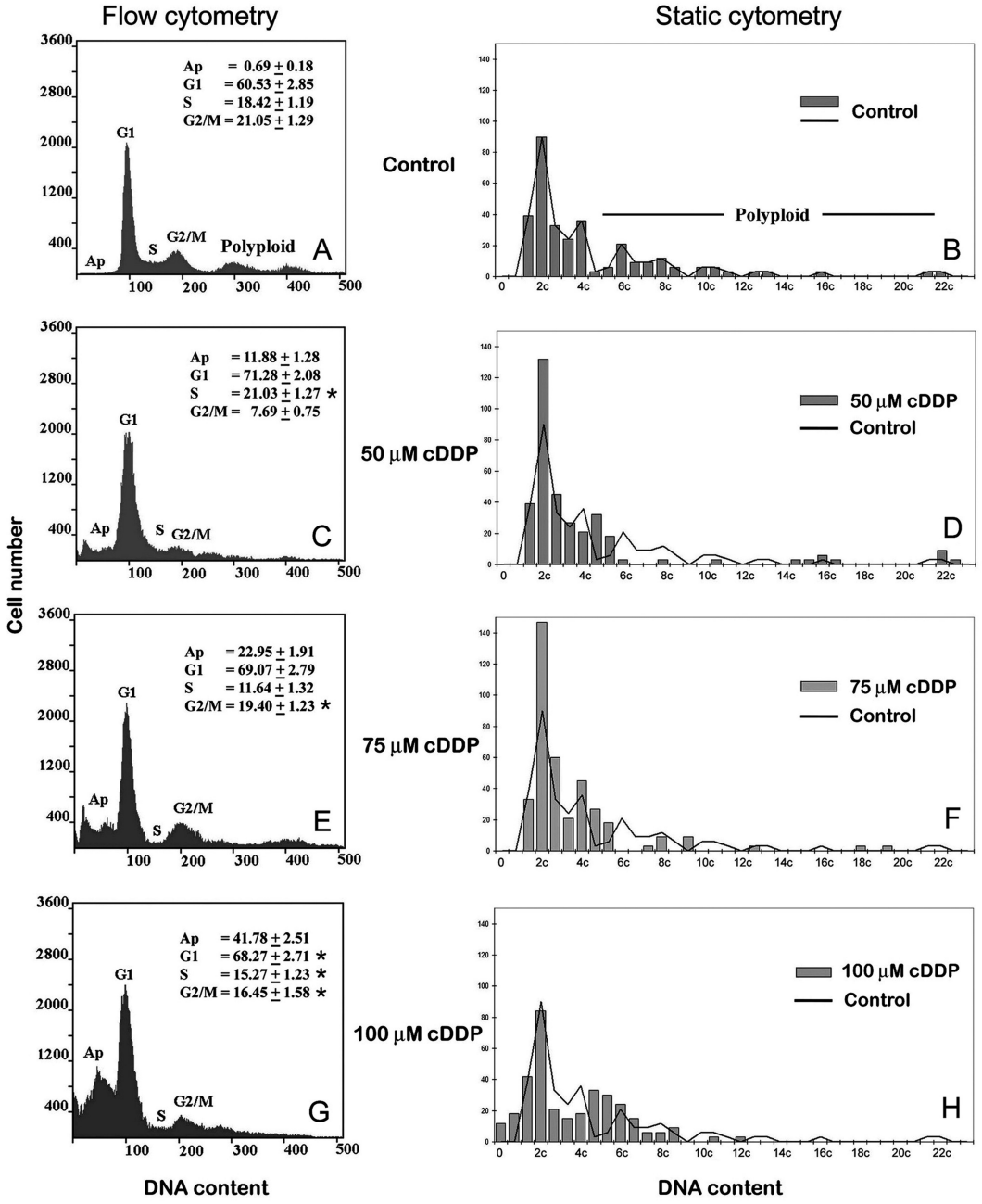

Fig. 1. Typical flow (**A, C, E, G**) and static (**B, D, F, H**) cytometric analyses of the DNA cellular content in control (**A, B**) and in cDDP-treated NIH/3T3 cells (**C, D:** 50 μM; **E, F:** 75 μM; **G, H:** 100 μM). In **B, D, F, H,** the curves represent the interpolation of the values of control frequency histograms. The analysis of histograms, in particular those relative to static cytometry, shows the dynamics of the appearance-disappearance of cells with high polyploid/aneuploid levels. The reported values represent the percentage (mean ± SEM of triplicate experiments) of cells in each phase of the cell cycle (G1, S, G2/M), calculated by excluding apoptotic fraction (Ap). The asterisks indicate the values that are not significantly different ($P > 0.05$ after Student's t-test) from the control.

values ranging from 6c to 14c (already evident at 50 µM cDDP), elements with ploidy values around 16c and 22c seemed to disappear, as a probable consequence of their involvement in degenerative phenomena (Fig. 1F). At 75 µM cDDP, the increase of protein content values of 8c cells could represent, in addition to G1 blocked octaploid cells, the shift of high polyploid cells in the proteolytic phase (Fig. 2C); for instance, 16c and 22c cells, increased at 50 µM cDDP, now appear to be drastically reduced (Fig. 1D, F).

As far as 100 µM cDDP treatment was concerned, it was possible to outline scarce effects on proliferative activity (Fig. 1G); nevertheless, in comparison to 50 and 75 µM conditions, cell death induction was more strongly deducible by the increase of sub-G1 cells derived from diploid and, in part, from 4c-8c polyploid cells (Fig. 1G). Moreover, treatment with 100 µM cDDP caused the loss of highly-ploidy cells (c > 12) (Fig. 1H); the appearance of DNA content values ranging from 4c to 6c in all treatment conditions (see static DNA content histograms in fig. 1) was probably indicative of DNA loss/degradation in cells with higher ploidy values. In fact, morphological analysis of still adherent cells prevailingly demonstrated the presence of patterns of cell degeneration, alternative to conventional apoptosis, especially in larger cells, with great alterations at both nuclear and cytoplasmic levels. The increase of sub-G1 protein values (Fig. 2D) could derive from the addition of degenerating polyploid cells to cell fragments (low protein values) of conventional apoptotic derivation.

Nuclear alterations

Besides cytostatic effects, cDDP induced different types of karyological modifications (e.g. small micronuclei, U/O-shaped nuclei, multilobulated nuclei, and apoptotic nuclei), the morphological features of which, after staining with the metachromatic fluorochrome Acridine Orange, are shown in figure 3, while the respective percentage values are reported in figure 4A.

Global analysis of the curves indicated that the various treatment conditions of NIH/3T3 cells induced some variability in the appearance/disappearance of the different nuclear changes (Fig. 4A). Concentrations of 50 µM cDDP determined the appearance of cells with small micronuclei (Fig. 3A), probably related to the perturbation of mitotic mechanisms (Fig. 3B,C).

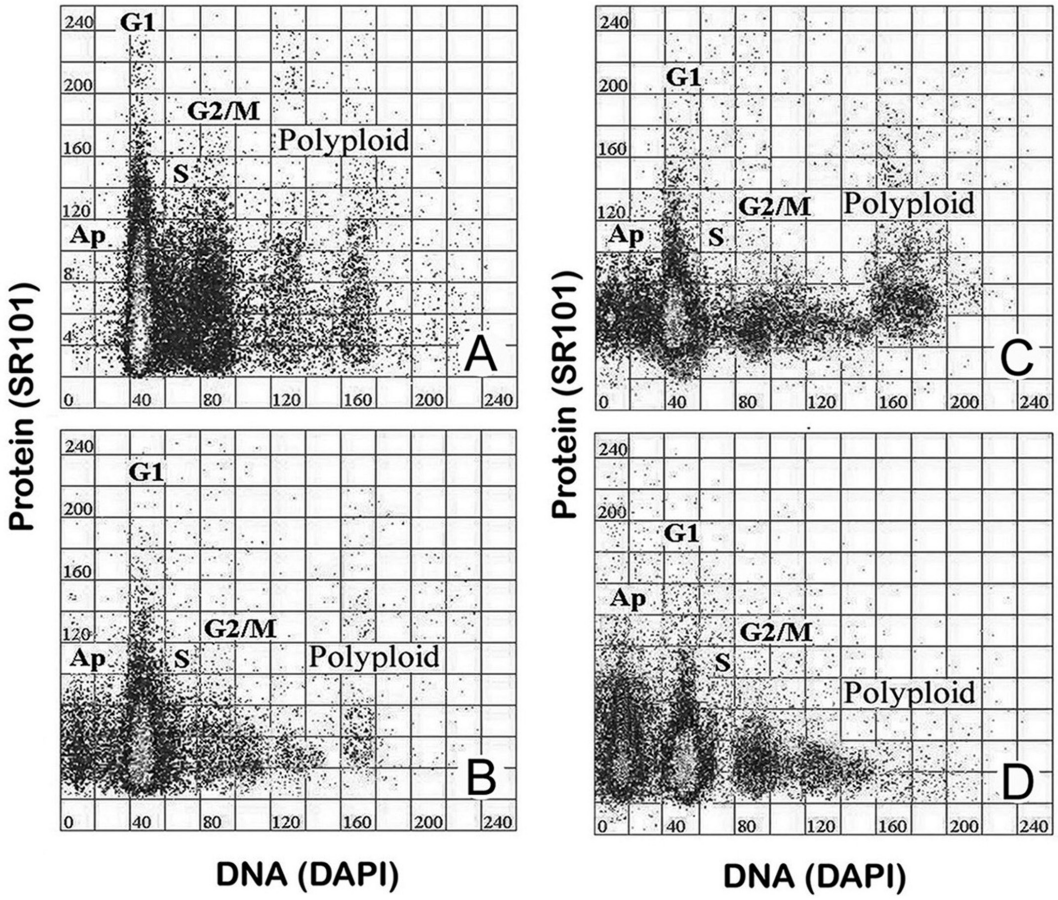

Fig. 2. Bivariate dot plots of DNA versus protein cell contents (flow cytometry after DAPI/SR101 staining) in control (**A**) and after cDDP treatment (**B:** 50 µM; **C:** 75 µM; **D:** 100 µM). The effects of cDDP at various concentrations on the cell protein content of the different subpopulations are shown.

By comparing figure 3a with figure 5d, it is possible to outline the different dimensions of micronuclei: bigger micronuclei are associated with other nuclear anomalies and changes, which characterize the more drastic drug treatment conditions (Fig. 3E,F, 5).

In fact, at higher concentrations, 75 µM and especially 100 µM, cDDP induced the formation of multilobulated nuclei with heterogeneous morphology (Fig. 3E,F). Moreover, 75 µM cDDP treatment conditions seemed to represent a situation in which notable dynamic changes at nuclear level appeared: there was a reduction in the number of small micronuclei and an increase of the appearance of furrowed nuclei and those with variable shapes (Fig. 3D, 4A). The latter may testify to the probable transition toward other anomalies, such as highly multilobulated and segmented nuclei. In figure 5, possible dynamic steps of nuclear lobulation/fragmentation with consequent formation of

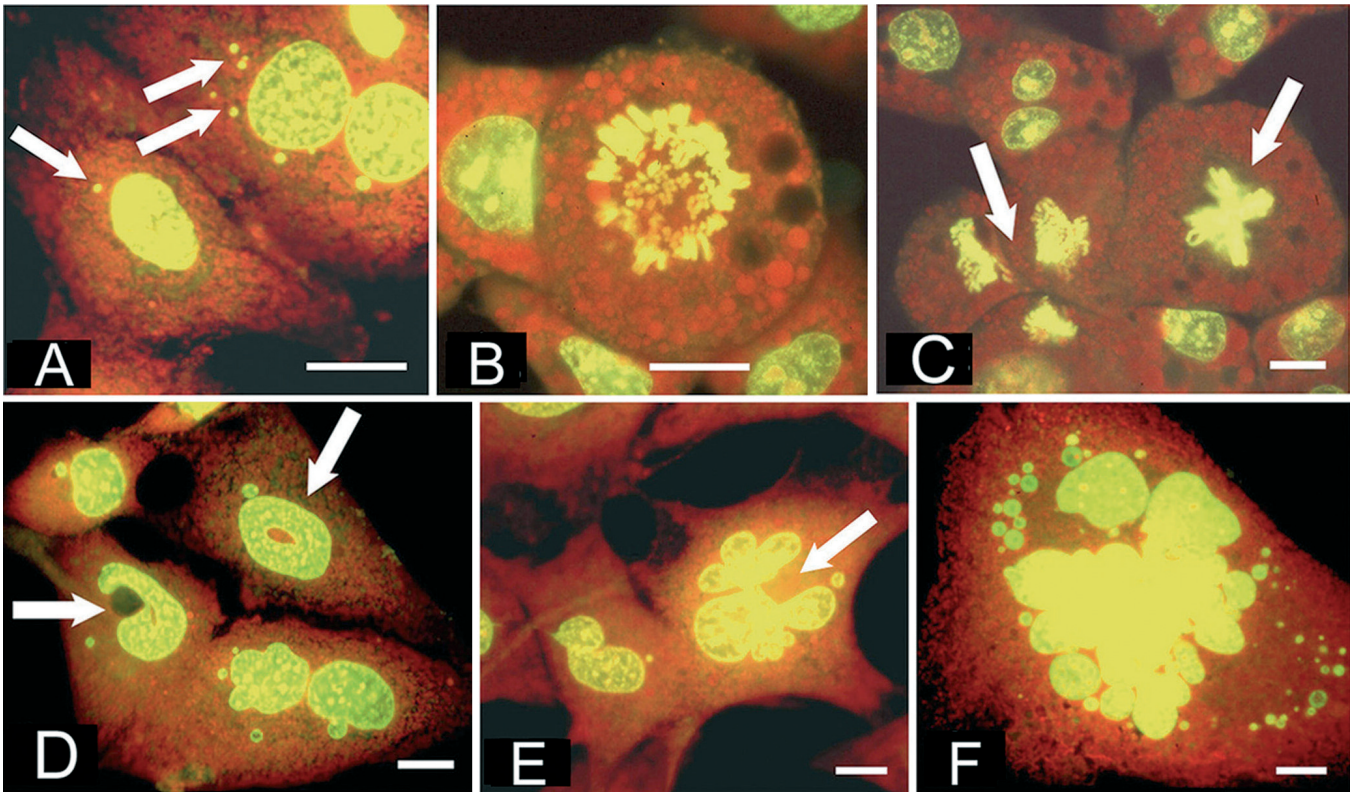

Fig. 3. Fluorescence microscopy of Acridine Orange-stained NIH/3T3 cells after cDDP treatment (**A, B, C:** 50 µM; **D,E:** 75 µM; F: 100 µM). **A.** Presence of small micronuclei (arrows). **B, C.** Mitotic anomalies (arrows). **D.** O- and U-shaped nuclei (arrows). **E.** Multilobulated nucleus (arrow). **F.** Nuclear hyper-fragmentation in a highly polyploid cell. Bars: 6 µm.

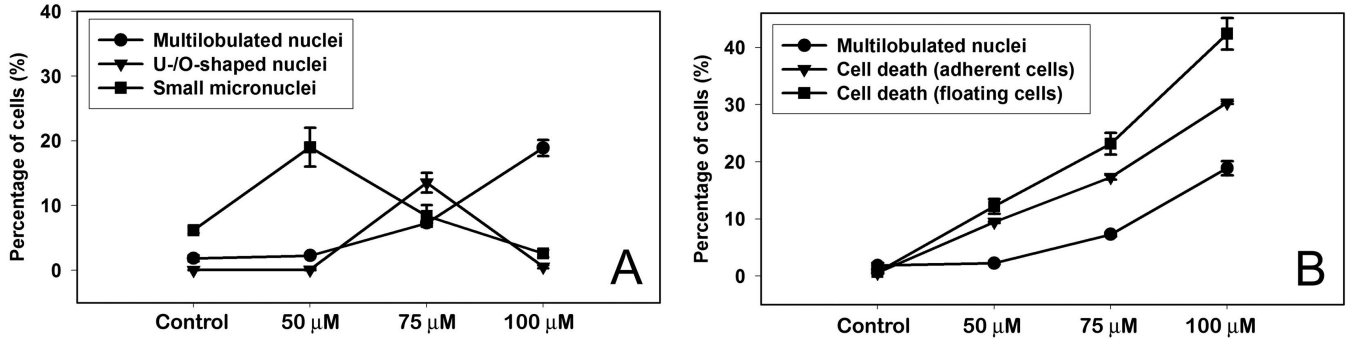

Fig. 4. Percentage distribution of main nuclear anomalies **(A)** and relationship between cell death phenomena (in adherent and floating cells) and the appearance of multilobulated nuclei **(B)**, in control and cDDP-treated NIH/3T3 cells. Data points represent mean ± SEM of triplicate experiments.

large micronuclei that are heterogeneous in size are shown. The process can originate with protrusions of the nuclear envelope (A), that tend to progressively move away (B) and are connected to the nucleus only by thin bridges of chromatin (C). Successively, micronuclei become detached and are free in the cytoplasm (D). Nuclear protrusions were also visible in electron microscopy micrographs (Fig. 6A,B); these alterations could cause fragmentation of the nucleus or the formation of micronucleations with large size.

The appearance of nuclear multilobulations and the presence of large micronucleations were particularly evident in polyploid cells showing the higher ploidy levels (Fig. 3F).

In the dynamics of nuclear lobulation/fragmentation events, the particular actin redistribution at the perinuclear area could play a role. In fact, treatment with the cytostatic drug caused not only variable concentration-dependent events of stress fibre distribution and peripheral actin depolymerization (not shown), but also the appearance of an actin ring around the nucleus (Fig. 6E). These contractile-like structures may possibly be involved in nuclear constriction phenomena (Fig. 6C,D,F) and can trigger the lobulation followed by the segmentation observed in the different cDDP treatment conditions. In figure 6C, nuclear furrows, which can be associated with the particular chromatin features (Fig. 6F), are shown.

These late nuclear changes, showing the highest incidence after 75-100 µM cDDP, especially affected the more adherent cells with high ploidy levels, which were of larger dimensions in comparison to the predominant cell population. These anomalies can represent a transition phase toward a way of cell death alternative to classical apoptosis. The number of cells with multilobulated nuclei appeared to be related to the increase of different cell death phenomena, prevailingly expressed by still adherent polyploid cells (Fig. 4B); this is evident especially after 100 µM cDDP treatment. Furthermore, in the present experimental conditions, the increase of classical apoptosis is present in both floating and adherent cells (Figs. 1G; 4B).

In cells with high ploidy levels, characterized by larger sizes with respect to the modal cell population, besides nuclear alterations, there were often degenerative patterns at cytoplasm level.

Cytoplasm alterations

In addition to the changes of protein content as expression of protoplasmic mass (Fig. 2), some structural modifications at cytoplasmic level, such as the

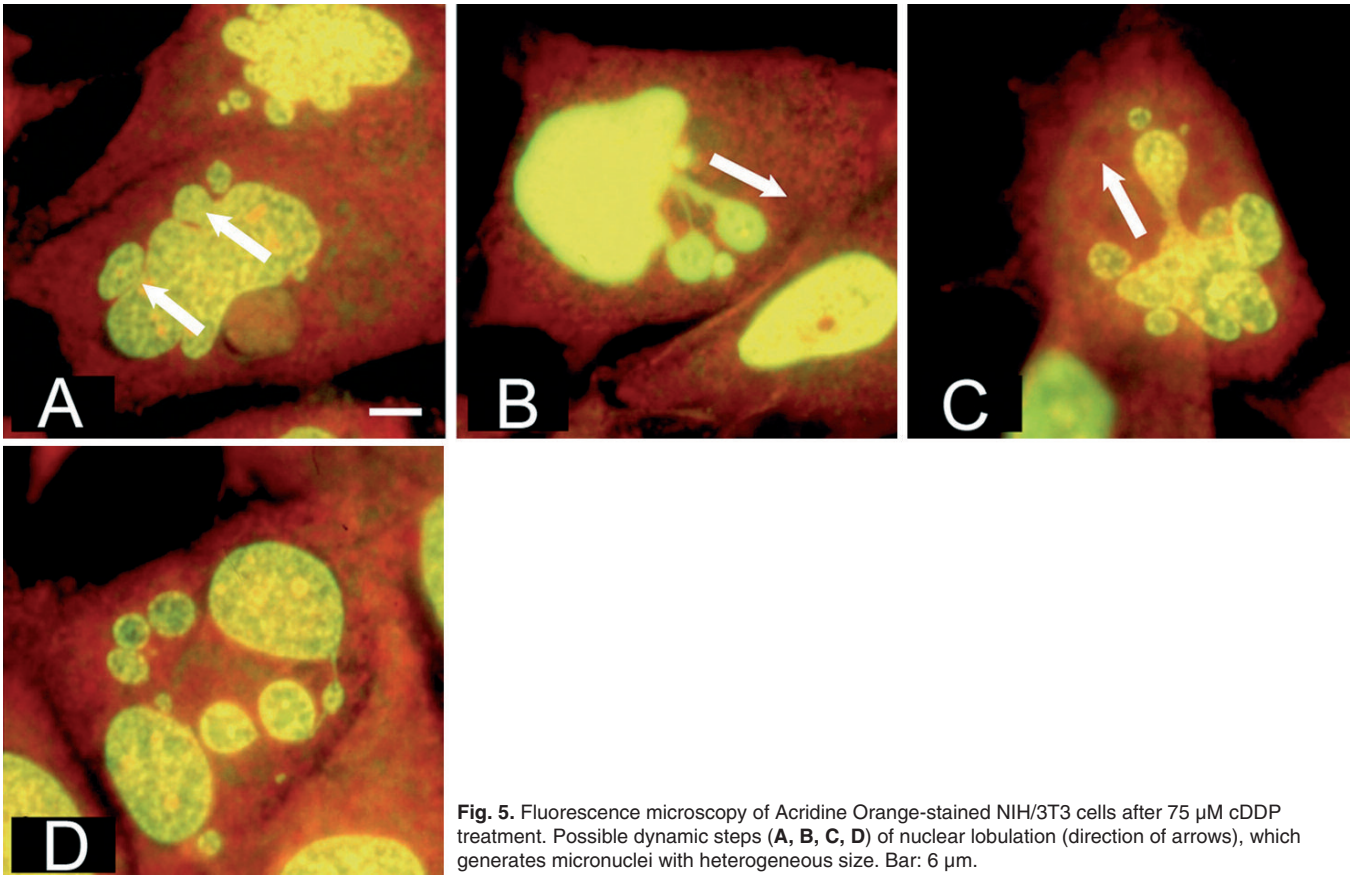

Fig. 5. Fluorescence microscopy of Acridine Orange-stained NIH/3T3 cells after 75 µM cDDP treatment. Possible dynamic steps (**A, B, C, D**) of nuclear lobulation (direction of arrows), which generates micronuclei with heterogeneous size. Bar: 6 µm.

presence of wide vacuolization areas, have been revealed after Acridine Orange (AO) staining, which permitted metachromatic distinction between nucleic acids (DNA – green fluorescence; RNA – red fluorescence), and lysosomes (bright red fluorescence). In figure 7, primary and secondary lysosomes appeared as heterogeneous size granules with a bright red fluorescence, different from that emitted by cytoplasmic RNA, in dependence of lysosome low pH. These morpho-cytochemical aspects were also integrated with ultrastructural analysis. Electron microscopy also showed events of cytoplasmic degeneration in polyploid cells (Fig. 6A). In figure 8, some aspects of these events were detectable, such as a high number of secondary lysosomes (Fig. 8A,B), the presence of autophagocytic phenomena (Fig. 8C), and the appearance of residual bodies and myelin figures

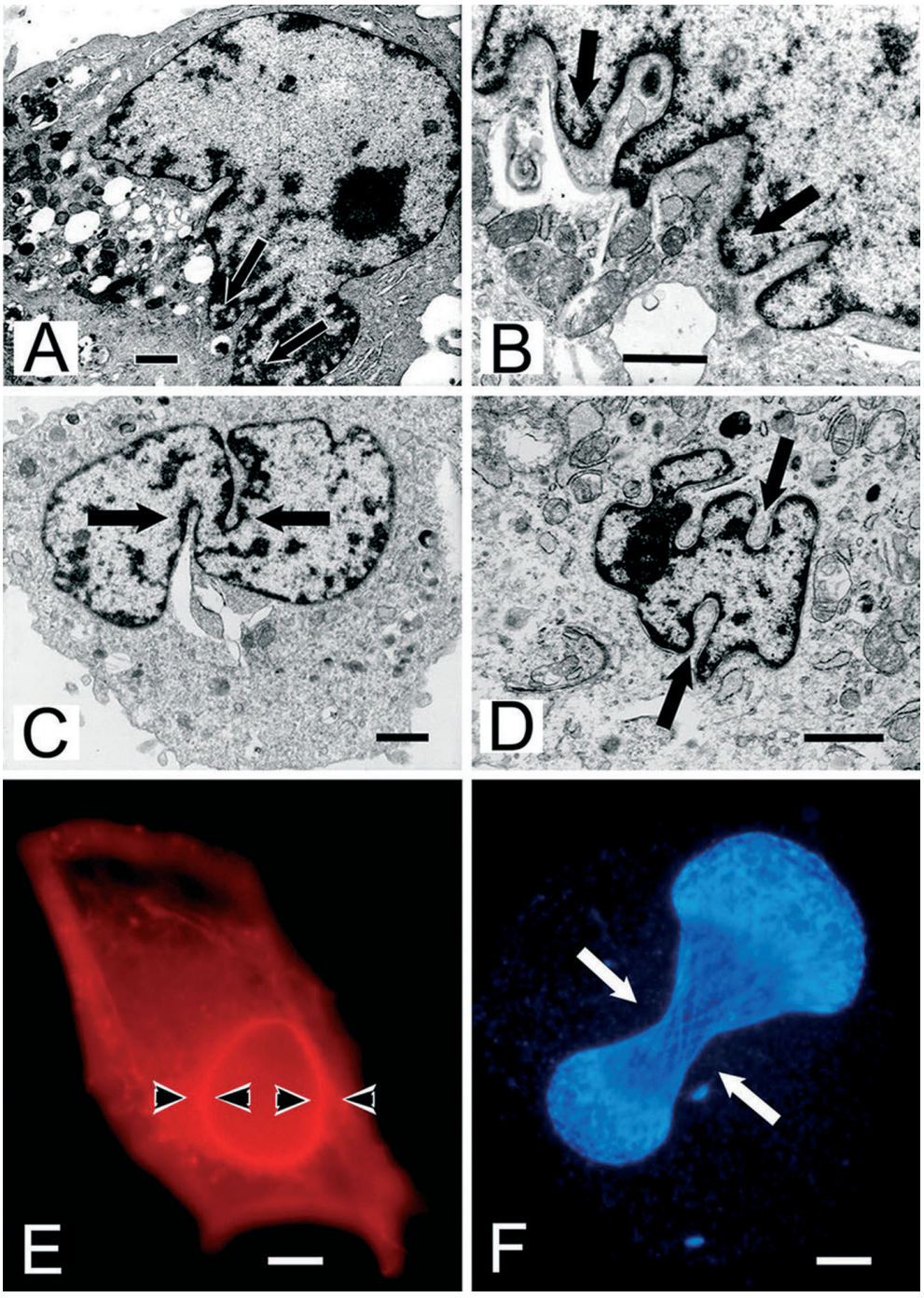

Fig. 6. Ultrastructural aspects (**A, B, C, D**) and fluorescence microscopy (**E, F**) of 75 μM cDDP-treated NIH/3T3 cells. Budding (**A, B**) and constriction (**C, D**) phenomena at nuclear level (arrows). **A.** Extensive cytoplasmic autophagocytic alterations in a cell with large nucleus (polyploid cell) are shown. **E.** Example of actin distribution (phalloidn – TRITC fluorochomization), at the perinuclear area, arranged as a ring-like structure (arrowheads). **F.** Effect of probable constrictional/torsional forces (arrows) at nuclear level (Hoechst 33342 fluorochromization). Bars: A-D, 1 μm; E, F, 6 μm.

(Fig. 8D). This is expression of intense autodegradation of organelles and endomembranes. Cells in advanced stages of degeneration (higher incidence after 100 µM cDDP treatment) showed the presence of electrondense vacuoles, deriving from the probable fusion of secondary autophagosomes (Fig. 8B). In some cases, these ultrastructural aspects were associated with the presence of electron-lucent vacuoles (Fig. 9B), which can represent nuclear fragments with degraded chromatin.

Areas with electron-lucent features were also visible at nuclear level, in the erniations of the nuclear envelope (Fig. 9A,C).

In AO-stained specimens, in comparison to main nuclei, some nuclear fragments appeared to be characterized by a dark green fluorescence (Fig. 7), as a possible consequence of partial chromatin degradation and scattering. These latter aspects seemed to provide further support for the ultrastructural findings (Fig. 9A,B,C,D).

Ultrastructural analysis also showed the persistence of intermediate filaments, organized into bundles in the cytoplasm (Figs. 8E, 9F) and present in degenerating nuclei (Fig. 9E).

Discussion

Although cell death is widely involved in several physiological and pathological processes, there is no clear documentation regarding the appearance of forms of cell degeneration that show features referable to neither apoptosis, autophagic cell death or necrosis. Cellular and molecular mechanisms involved in these alternative forms of cell death are still not well-known, so that, in some pathologies the pharmacological or genetic modulation of only the conventional apoptotic way could represent an inefficient strategy when alternative forms of cell death appeared. Some situations of programmed cell death with features different to those

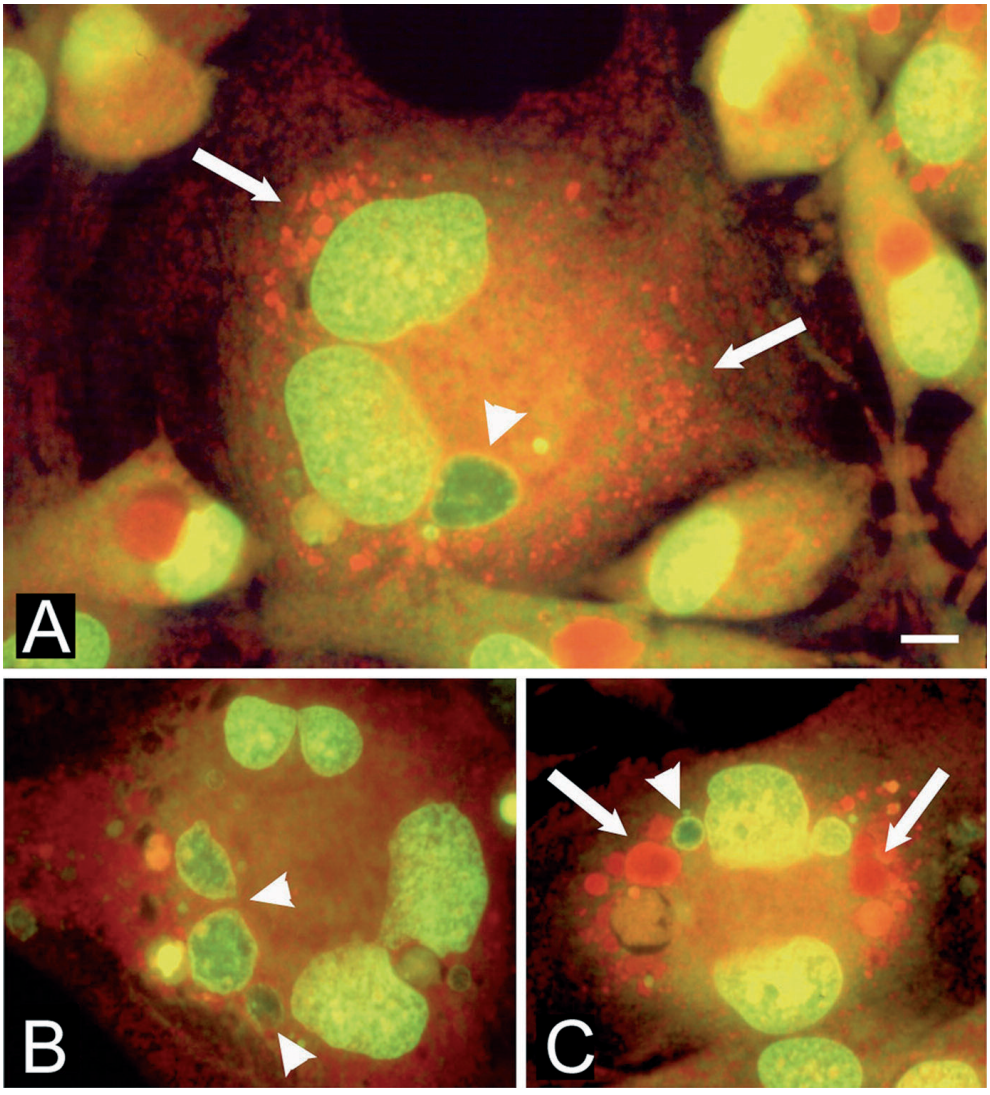

Fig. 7. Acridine Orange fluorochromization of high polyploid NIH/3T3 cells. Plurinuclearity and nuclear fragmentation appear to be correlated with strong cytoplasmic alterations. At cytoplasm level, the fluorochrome stains diffused **(A)** and wide **(C)** vacuoles (arrows) with acidic content (bright red fluorescence). At nuclear level **(A, B, C)**, in comparison to main nuclei, in some fragments (arrowheads), the chromatin appears to be characterized by a dark green fluorescence, indicative of a possible DNA degradation. Bar: 6 µm.

of classical apoptosis have been described, and in part referred to as necrosis, because of their morphological features of cytoplasmic vacuolization and mitochondrial swelling, and the absence of effects by caspase inhibitors (Sperandio et al., 2000).

However, accumulating evidence suggests that programmed cell death is not confined to apoptosis, but that cells arrive at active self-destruction in different

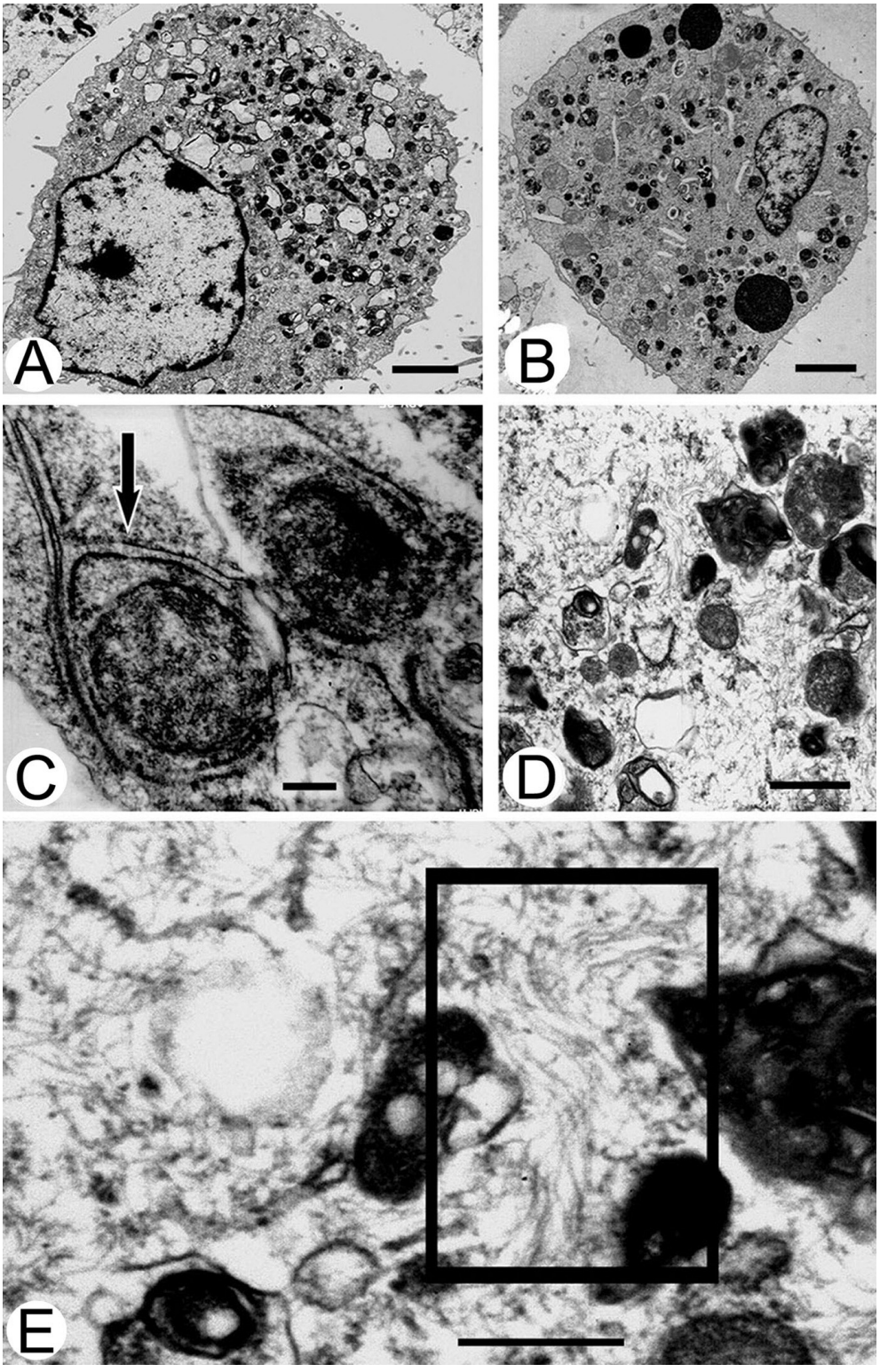

Fig. 8. TEM micrographs relative to cytoplasmic events of cell degeneration in 100 μM cDDP-treated NIH/3T3 cells. **A, B.** Presence of vacuolization and secondary lysosomes. **C.** Endomembranes surrounding a degenerating mitochondrion (arrow). **D.** Residual bodies. **E.** Higher magnification of image in **D**: in some areas of the cytoplasm, it is possible to find bundles of intermediate filaments (frame). Bars: A, B, 1 μm; C, E, 0.25 μm; D, 0.5 μm.

ways, as reflected by different morphology: condensation prominent, type I or apoptosis; and autophagy prominent, type II. In particular, the boundary between apoptosis and autophagic cell death has not been definitively established, and an overlap between these two types of cell death exists; apoptosis can begin with autophagy, autophagy can end with apoptosis (Lockshin and Zakeri 2004).

In our cell model, composed of sub-populations with different ploidies, treatment with cDDP is able to induce cell death phenomena referable to the two types of programmed cell death. It is interesting to note that cell populations prevailingly showing the two forms of cell death are different: in particular, cells of the predominant population (2c - 4c DNA content: highly-proliferating cells) tend to die by apoptosis, while aneuploid/polyploid cells (4c - 24c DNA content) tend to die by a form of autophagic death. As far as

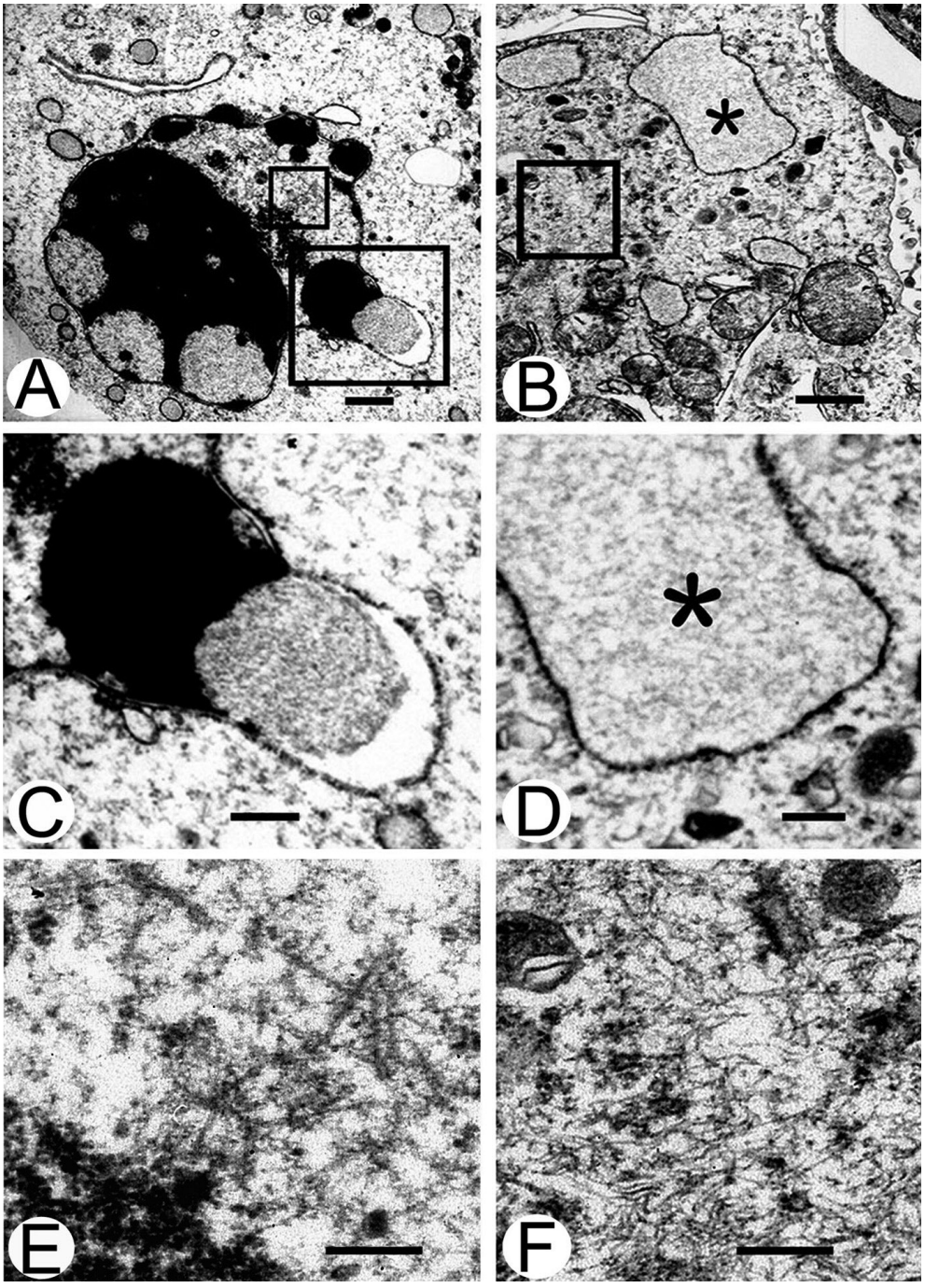

Fig. 9. TEM micrographs relative to nuclear (**A, C, E**) and cytoplasmic (**B, D, F**) degenerative events in 100 μM cDDP-treated NIH/3T3 cells. **A.** Patterns of chromatin hypercondensation and degradation. **C, E.** High magnifications of framed panels in **A. C.** Protrusion of the nuclear envelope in a transition area of hypercondensed/degraded chromatin. **E.** Persistence of intranuclear intermediate filaments. **D, F.** High magnification of particulars in **B. D.** Wide vacuole (asterisk) with electron-lucent content (the same kind of vacuoles is also visible in the cytoplasm in **A**), that appears similar to the material in the nuclear protrusion in **C. F.** Area of the cytoplasm (frame in **B**) with an intricate network of intermediate filaments near to degenerating organelles. Bars: A, B, 1 μm; C, 0.5 μm; D, E, F, 0.25 μm.

conventional apoptotic cell death is concerned, flow cytometry data demonstrate that its incidence is primarily related to drug concentration. During autophagic cell death, the various experimental conditions seem to cause not only evident cytoplasmic changes, in part supported by the decrease of the protein mass, but also the appearance of different nuclear anomalies, which, in some cases, can lead to situations partially common to type I apoptosis: in the same cell, chromatin hypercondensation events and autophagocytic phenomena have been observed. The reduction of proteinic mass at different ploidy levels could be attributed to the inhibition of transcription and to proteolytic mechanisms connected with the direct and indirect drug action, respectively (Siddik, 2003). As far as the specific effects of the different cDDP concentrations are concerned, the dose of 50 μM caused a notable increase in micronucleation phenomena. Although several mechanisms can be responsible for chromatin segregation in the cytoplasm (Stich and Rosin, 1984), the presence of micronuclei can also depend on the proliferative activity of the cells and can be responsible for the appearance of aneuploid cells (Nusse and Kramer, 1984). Micronuclei can originate from acentric fragments or whole chromosomes as a consequence of aneugenic or clastogenig damages (Barni et al.,1992). The presence of unsegregated genetic material (micronuclei), multinucleation and polyploidization can represent biological situations in which the control of both proliferative activity and the onset of programmed cell death can be highly impaired. By analyzing static and flow cytometry data, 50 μM cDDP causes the decrease of 6c and 8c values: cells with this DNA content are probably cytokinetically unstable, a condition which can lead to their loss by mechanisms of cell death. Alternatively, phenomena of anomalous polyploid cell division (appearance of multipolar spindles) can contribute to the reduction of the number of hexaploid and octaploid cells. In fact, amongst the various effects induced by cDDP, fluorescence microscopy demonstrated the presence of tripolar and tetrapolar mitoses. By means of these mitotic mechanisms, which can occur in polyploid cells, restitution of 4c cells can take place. Other Authors (Illidge et al., 2000) have demonstrated a reciprocal relationship between the polyploid cells and the diploid stem component, decreased during polyploid cell formation and restituted by depolyploidization after giant cell segmentation. Therefore, the formation of 4c cells derived from 6c and 8c cells could represent a biological process of resistance and survival, carried out by polyploid cells, alternative to death phenomena induced by cDDP treatment. Furthermore, at 50 μM dose, the decrease of cells with 8c DNA content is correlated with the reduction of the 4c peak (G2/M phase in flow cytometry), which is representative of the diploid proliferating cells in the G2/M phase and can be partly constituted by tetraploid cells in the G1 phase. In contrast with the disappearance of 10c-14c cells, the persistence of 16c and 22c polyploid cells, after mild stimulation, emphasizes the heterogeneous composition of the NIH/3T3 cells here used, characterized by the presence of sub-populations with different sensitivity to the cytotoxicity of the drug and corresponding survival capacity. This situation could involve no immediate effects of cDDP in the induction of cell death [e.g. during the cell cycle(s) subsequent to that in which the cell was initially affected]. Moreover, the mode of cell death (e.g. apoptosis or autophagy) could be distinguished in relation to the cell cycle phase in which it is induced (interphasic or mitotic cell death) (Halicka et al., 1997). Treatment with 75 μM cDDP represents a condition in which there are notable dynamic changes, at both nuclear and cytoplasmic levels. The number of small micronuclei is reduced, while other nuclear anomalies are favoured, such as nuclei with altered morphology (U- and O-shaped). Similar features have already been observed amongst the nuclear changes induced by cisplatin in C6 glioma cells (Krajčí et al., 2006). In our cell model, these alterations could represent transition stages toward more drastic karyological alterations. Cells with multilobulated and often segmented nuclei are involved in advanced stages of degeneration, evident after 75 μM cDDP and especially after 100 μM cDDP treatment. Analysis of static cytofluorometric profiles, relating to 75 μM cDDP, demonstrates a decrease in values corresponding to DNA content around 22c and the appearance of DNA content values ranging from 18c to 20c, probably representative of degenerating 22c cells. After 100 μM cDDP treatment, the percentage incidence of multilobulated nuclei may be related to the disappearance of polyploid cells with DNA content higher than 12c. Furthermore, the analysis of the static cytofluorometric profile permits us to show how the degeneration of these polyploid cells causes an accumulation of values ranging from 4c to 10c, not otherwise justifiable by a recovery of proliferative activity.

Referring to the drastic changes of polyploid cells with highly segmented nuclei, large micronuclei that seem to originate from protrusions of the nuclear envelope are present. In this kind of dynamic event, actin reorganization phenomena could play a role: fluorescence microscopy analysis demonstrates that cDDP treatment determines actin reorganization, with redistribution at perinuclear area. This phenomenon can contribute to the organization of structures with contractile function, involved in the mechanisms of nucleus lobulation and segmentation, resulting in both multinucleation and/or formation of large micronuclei. A similar role for actin has been described during type I apoptosis (Spano et al., 2000). In this form of cell death, proteolytic degradation of the nuclear lamina can also contribute to changes at nuclear level (Rao et al., 1996).

Our observations permit the outlining of two alternative ways of death. In the first one, which characterizes classical apoptosis (type I) and involves the predominant cell population (2c - 4c) of the culture, the chromatin is degraded, following the typical

phenomena widely described in literature. In the second way, especially involving polyploid cells, there are mechanisms that lead to the formation of nuclear fragments (and/or large micronuclei), which can be expelled or degraded within the cell. On the whole, our experimental evidence seems to demonstrate that these nuclear degeneration phenomena are strictly related to the extensive cytoplasmic modifications, observed especially in polyploid cells. These changes are represented by wide areas of vacuolization, spread throughout the cytoplasm, and with small or large vacuoles with acidic content, metachromatically stained with Acridine Orange (Zelenin, 1999). Transmission electron microscopy of NIH/3T3 cells demonstrates, especially after 100 µM cDDP stimulation, a cytoplasm characterized by the presence of secondary lysosomes and residual bodies. At higher magnification, it is possible to detect the presence of myelin figures, indicative of a notable autodegradation of endomembranes and organelles. In fact, degenerating mitochondria, within autophagosomes, are evident. The fusion of secondary phagosomes could justify the presence of the large electrondense vacuoles, which are sometimes observed. Further information during the self-degradation of the cell can be obtained from the measurement of the cell protein content, which appeared significantly reduced at this drug dose.

Electronlucent vacuolisations, which were found mainly in cells with highly altered nuclei, could represent areas of chromatin degradation, also detectable in fluorescence microscopy.

These observations agree with the literature on autophagic cell death, the expression of which implies the digestion of nuclear fragments, beyond the degradation of the Golgi apparatus, endoplasmic reticulum, ribosomes, and organelles in general (Bursch, 2001; Lockshin and Zakeri 2004). Morphological and biochemical studies have demonstrated that autophagy is a multi-step process, in which, initially, various organelles and cytoplasm areas are surrounded by endomembranes with consequent formation of autophagosome (Munafò and Colombo, 2001; Martinet et al., 2006). Furthermore, in autophagic cell death (type II), cytoskeletal integrity in the late stages of the phenomenon is necessary, while initial steps of type I apoptosis are already associated with actin depolymerization and intermediate filament degradation (Tinnemans et al., 1995; Spano et al., 2000). In type II cell death, these components are redistributed and partially preserved (Bursch et al., 2000). This is also demonstrated in our experiments, in which 100 µM cDDP, which causes the highest incidence of type II degenerative phenomena, does not lead to complete actin microfilament depolymerization. To further support the cytoskeleton role in alternative cell death phenomena, there is the persistence of intermediate filaments, which we observed in cells with evident autolytic signs at cytoplasm level. This is in agreement with current opinions that consider intermediate filaments, during autophagocytosis, as well as microfilaments, essential for the initial formation of autophagosomes, while the consequent fusion with lysosomes seems to depend on microtubules (Blommaart et al., 1997). These aspects outline how lysosomes play a fundamental role in type II cell death phenomena, in which they could be important mediators of the death program, even by considering their protease release ability, such as cathepsin (Salvesen, 2001).

Our data demonstrated that the same drug, at different concentrations, was able to induce variable mechanisms of cell degeneration relating to cytokinetic activity, cell size and ploidy. More actively proliferating cells (2c - 4c DNA content) died throughout typical apoptosis, while polyploid cells degenerated mainly by means of mechanisms of alternative cell death, partly referable to autophagic apoptosis. In this kind of cell death, chromatin hypercondensation events are not always evident. This fact could perhaps be related to the dynamics of the aforementioned nuclear changes leading to the formation of large micronuclei. Furthermore, in our experience and in other cell models, micronucleated cells (without DNA condensation) show DNA fragmentation, as revealed by TUNEL reaction (Sciola et al., 2003; Spano et al., 2007). These cellular aspects can be interpreted by considering that cells with unstable and damaged genome (such as aneuploid/polyploid cells) can express altered levels of cell regulators and partially disable some mechanisms of classical apoptosis, following an alternative way of death, also starting from abnormal mitoses.

These findings, and the other morpho-cytochemical and ultrastructural features, typical of programmed autophagic cell death, do not exclude that this kind of degeneration and conventional apoptosis are not reciprocally exclusive phenomena. The two forms of death can occur not only in the same culture (as we demonstrate), but also in the same cell, perhaps in different stages of cellular degeneration.

In conclusion, in our cell model, cells can use different ways or modalities of expression to activate their self-destruction, although a possible reciprocal conversion between apoptosis and autophagic cell death, as a form of "hybrid death", may occur. Referring to in vivo conditions, in our opinion, forms of autophagic cell death could be involved in the elimination of large polyploid cells, in order to reduce cellular dimension and to facilitate the consequent involvement of the scavenger cell system, that are normally operating in the organism.

References

Andreassen P.R., Lohez O.D., Lacroix F.B. and Margolis R.L. (2001). Tetraploid state induces p53-dependent arrest of non transformed mammalian cells in G1. Mol. Biol. Cell 12, 1315-1328.

Barni S., Porcelli F., Scherini E. and Spadari S. (1992). Induction of karyological damage by bleomycin in polyploidizating rabbit hepatocytes. Anticancer Res. 12, 521-528.

Baroja A., de la Hoz C., Alvarez A., Ispina A., Bilbao J. and De Gandarias J.M. (1996). Genesis and evolution of high ploidy tumour cells evaluated by means of the proliferation markers p34(cdc2),

cyclin B1, PCNA and 3[H]-thymidine. Cell Prolif. 29, 89-100.

Baroja A., de la Hoz C., Alvarez A., Vielba R., Sarrat R., Arechaga J. and De Gandarias J.M. (1998). Polyploidization and exit from cell cycle as mechanisms of cultured melanoma cell resistance to methotrexate. Life Sci. 62, 2275-2282.

Blommaart E.F., Luiken J.J.F.P. and Meijer A.J. (1997). Autophagic proteolysis control and specificity. Histochem. J. 29, 365-385.

Böhm N. and Sandritter W. (1975). DNA in human tumors: a cytophotometric study. Curr. Top. Pathol. 60, 151-219.

Bursch W., Hochegger K., Torok L., Marian B., Ellinger A. and Schulte-Hermann R. (2000). Autophagic and apoptotic types of programmed cell death exhibit different fates of cytoskeletal filaments. J. Cell Sci. 113, 1189-1198.

Bursch W. (2001). The autophagosomal-lysosomal compartment in programmed cell death. Cell Death Differ 8, 569-581.

Castedo M., Coquelle A., Vivet S., Vitale I., Kauffmann A., Dessen P., Pequignot M.O., Casares N., Valent A., Mouhamad S., Schmitt E., Modjtahedi N., Vainchenker W., Zitvogel L., Lazar V., Garrido C. and Kroemer G. (2006). Apoptosis regulation in tetraploid cancer cells. EMBO J. 25, 2584-2595.

Ciciarello M., Mangiacasale R., Casenghi M., Limongi M.Z., D'Angelo M., Soddu S., Lavia P. and Cundari E. (2001). p53 displacement from centrosomes and p53-mediated G1 arrest following transient inhibition of the mitotic spindle. J. Biol. Chem. 276, 19205-19213.

Dejmek A., Stromberg C., Wikstrom B. and Hjerpe A. (1992). Prognostic importance of the DNA ploidy pattern in malignant mesothelioma of the pleura. Anal. Quant. Cytol. Histol. 14, 217-221.

Halicka H.D., Seiter K., Feldman E.J., Traganos F., Mittelman A., Ahmed T. and Darzynkiewicz Z. (1997). Cell cycle specificity of apoptosis during treatment of leukaemias. Apoptosis 2, 25-39.

Illidge T.M., Cragg M.S., Fringes B., Olive P. and Erenpreisa J.A. (2000). Polyploid giant cells provide a survival mechanism for p53 mutant cells after DNA damage. Cell Biol. Int. 24, 621-633.

Klein G. and Klein F. (1985). Evolution of tumors and the impact of molecular oncology. Nature 315, 190-195.

Krajčí D., Mares V., Lisá V., Bottone M.G. and Pellicciari C. (2006). Intranuclear microtubules are hallmarks of an unusual form of cell death in cisplatin-treated C6 glioma cells. Histochem. Cell Biol. 125, 183-191.

Liautaud-Roger F., Dufer J. and Coniux P. (1990). Tetraploid cycle in ageing solid tumours. Cell Tissue Kin. 23, 261-269.

Lockshin R. and Zakeri Z. (2004). Apoptosis, autophagy, and more. Int. J. Biochem. Cell Biol. 36, 2405-2419.

Martinet W., De Meyer R.Y., Andries L., Herman A.G. and Hockx M.M. (2006). In situ detection of starvation-induced autophagy. J. Histochem. Cytochem. 54, 85-96.

Melchiorri C., Bolondi L., Chieco P., Pagnon M., Gramantieri L. and Barbara L. (1994). Diagnostic and prognostic value of DNA ploidy and cell nuclearity in ultrasound-guided liver biopsies. Cancer 74, 1713-1719.

Mora J., Lavarino C., Alaminos M., Cheung N.K., Rios J., de Torres C., Illei P., Juan G. and Gerald W.L. (2007). Comprehensive analysis of tumoral DNA content reveals clonal ploidy heterogeneity as a marker with prognostic significance in locoregional neuroblastoma. Genes Chromosomes Cancer 46, 385-396.

Munafò D.B. and Colombo M.I. (2001). A novel assay to study autophagy: regulation of autophagosome vacuole size by amino acid deprivation. J. Cell Sci. 114, 3619-3629.

Nguen H.G. and Ravid K. (2006). Tetraploidy/aneuploidy and stem cell in cancer promotion: the role of chromosome passenger proteins. J. Cell. Physiol. 208, 12-22.

Nishigaki K., Thompson D., Yugawa T., Rulli K., Hanson C., Cmarik J., Gutkind S., Teramoto H. and Ruscetti S. (2003). Identification and characterization of a novel Ste20/germinal center kinase-related kinase, polyploid-associated protein kinase. J. Biol. Chem. 15, 13520-13530.

Nusse M. and Kramer J. (1984). Flow cytometric analysis of micronuclei found in cells after irradiation. Cytometry 5, 20-25.

Rao L., Perez D. and White E. (1996). Lamin proteolysis facilitates nuclear events during apoptosis. J. Cell Biol. 135, 1441-1455.

Salvesen G.S. (2001). A lysosomal protease enters the death scene. J. Clin. Invest. 107, 21-22.

Sciola L., Spano A., Monaco G., Bottone M.G. and Barni S. (2003). Different apoptotic responses and patterns in adhering and floating neoplastic cell cultures: effects of microtubule antagonists. Histochem. Cell Biol. 119, 77-90.

Siddik Z.H. (2003). Cisplatin: mode of cytotoxic action and molecular basis of resistance. Oncogene 22, 7265-7279.

Spano A., Sciola L., Monaco G. and Barni S. (2000). Relationship between actin microfilaments and plasma membrane changes during apoptosis of neoplastic cell lines in different culture conditions Eur. J. Histochem. 44, 255-267.

Spano A., Monaco G., Barni S. and Sciola L. (2007). Expression of cell kinetics and death during monocyte-macrophage differentiation: effects of Actinomycin D and Vinblastine treatments. Histochem .Cell Biol. 127, 79-94.

Sperandio S., de Belle I. and Bredesen D.E. (2000). An alternative, non apoptotic form of programmed cell death. Proc. Natl. Acad. Sci. USA 97, 14376-14381.

Stich H.F. and Rosin M.P. (1984). Micronuclei formation in exfoliated human cells as a tool for studies in cancer risk and cancer intervention. Cancer Lett. 22, 241-253.

Strathdee G., Sansom O.J., Sim A., Clarke A.R. and Brown R. (2001). A role for mismatch repair in control of DNA ploidy following DNA damage. Oncogene 20, 1923-1927.

Tinnemans M.M.F.J., Lenders M.H.J.H., ten Velde G.P.M., Ramaekers F.C.S. and Schutte B. (1995). Alterations in cytoskeletal and nuclear matrix-associated proteins during apoptosis. Eur. J. Cell Biol. 68, 35-46.

Un F. (2007). G1 arrest induction represents a critical determinant for cisplatin cytotoxicity in G1 checkpoint-retaining human cancers. Anticancer Drugs 18, 411-417.

Yildirim-Assaf S., Coumbos A., Hopfenmüller W., Foss H.D., Stein H. and Kühn W. (2007). The prognostic significance of determining DNA content in breast cancer by DNA image cytometry: the role of high grade aneuploidy in node negative breast cancer. J. Clin. Pathol. 60, 649-655.

Zelenin A.V. (1999). Acridine Orange as a probe for cell and molecular biology. In: Fluorescent and luminescent probes for biological activity. Mason W.T. (ed.). Academic Press. London. pp 117-135.

Zong Z.P., Fujikawa-Yamamoto K., Ota T., Murakami M., Li A.L., Yamaguchi N., Tanino M. and Odashima S. (1998). Apoptotic cell death of high polyploid cells in a cultured sarcoma cell line. Cell Struct. Funct. 23, 231-237.

Accepted December 24, 2007